Close-coupling and distorted-wave calculations for electron-impact excitation of the ($5p^5 6p$) states of xenon

K. Bartschat

Department of Physics and Astronomy,

Drake University, Des Moines, IA 50311, USA

A. Dasgupta

Plasma Physics Division, Naval Research Laboratory, Washington, D.C. 20375, USA

D.H. Madison

Physics Department, University of Missouri-Rolla, Rolla, MO 65401, USA

(Dated: April 6, 2004)

Abstract

We report on a series of calculations for electron impact-excitation of the $(5p^5)6p$ states in xenon from the ground state $(5p^6)^1S_0$. As in previous calculations for other noble-gas targets, we find strong evidence of channel coupling for all incident energies considered (between threshold and 200 eV). Although qualitative agreement with the experimental results of Fons and Lin (Phys. Rev. A **58** (1998) 4603) is achieved, severe quantitative discrepancies of sometimes more than a factor of two remain.

PACS numbers: 34.80.Dp

I. INTRODUCTION

Electron scattering from xenon atoms is an important process in laser, lighting, and plasma technology. Early measurements were summarized by Fons and Lin [1] who published a complete set of new experimental data for electron impact excitation cross sections from the ground state $(5p^6)^1S_0$ to the ten fine-structure states associated with the $(5p^5 6p)$ configuration. After subtracting cascade effects in the optical emission function measurements and accounting for the strong pressure dependence in typical experimental setups, they compared their data for a few transitions with predictions from an R-matrix (close-coupling) calculation by Nakazaki *et al.* [2]. Already in a previous publication [3], the latter authors had outlined some of the difficulties encountered in numerical calculations for these processes, generally consisting of both the complexity of the target description and the need to account for strong channel coupling, especially in the low-energy near-threshold regime that is dominated by resonance effects.

The near-threshold resonance problem was recently investigated in more detail by Grum-Grzhimailo and Bartschat [4] who looked at angle-integrated and angle-differential cross sections for electron-impact excitation of the $(5p^5 6s)$ states. One of the by-products of their work was a relatively accurate (in terms of energies and oscillator strengths) description of the lowest 21 target states of xenon. The latter was achieved mostly by generating a $6d$ pseudo-orbital to improve the description of the odd-parity states, and by optimizing the 6p orbital on the lower six members of the $(5p^5 6p)$ manifold, i.e., the states associated with the $(5p^5)^2P_{3/2}$ core of Xe^+.

In light of the data needs not only for the near-threshold region but also for higher impact energies, we decided to continue our previous work on electron collisions with krypton [5, 6] and argon [7–9] atoms by applying various distorted-wave and close-coupling approaches to the e−Xe collision problem. By performing both close-coupling and distorted-wave calculations, using the same one-electron orbitals, we can explore the sensitivity of the results to channel-coupling effects. Finally, we hoped it to be straightforward to generate results for the entire energy regime of interest by combining low-energy close-coupling and high-energy first-order distorted-wave results. As will be shown below, however, this is not always possible, due to the apparent importance of higher-order effects even at high impact energies.

In the next section, we briefly describe the numerical methods, which have been outlined

in more detail in previous calculations listed in the references. We then discuss the results before drawing some conclusions and providing an outlook to future work on this type of collision processes.

II. THEORETICAL MODELS

The semi-relativistic R-matrix method used in the present work is essentially the same as described by Zeman and Bartschat [10, 11], except for the improved structure description given by Grum-Grzhimailo and Bartschat [4]. The 43-state model (to be labeled RM43 below) used in the latter calculation closely coupled the 31 states of neutral xenon with configurations $5p^6$, $5p^5 6s$, $5p^5 6p$, $5p^5 5d$, and $5p^5 7s$, as well as 12 pseudo-states generated from the $5p^5 \bar{6}d$ configuration. Here $\bar{6}d$ denotes a pseudo-orbital that was optimized on the description of selected members of the odd-parity spectrum. The latter target description was generated with the multi-configuration MCHF code of Froese Fischer *et al.* [12]. In a smaller 15-state calculation (RM15), we used just the states generated from the configurations $5p^6$, $5p^5 6s$, and $5p^5 6p$, and finally dropping the four states with configuration $5p^5 6s$ yielded the minimal 11-state close-coupling approach (RM11) for the transitions of interest. Differences in the results obtained with the same target description but a different number of coupled states provides an indication of the importance of channel-coupling effects.

We then used the Belfast suite of semi-relativistic R-matrix codes [13] to perform calculations for electron collisions with Xe atoms initially in their $(5p^6)^1S_0$ ground state. In the RM11 and RM15 calculations, the R-matrix radius was set to $30\,a_0$ and 40 continuum orbitals per angular momentum were used to represent the projectile inside the R-matrix box. This allowed us to push these calculations to incident energies up to 140 eV. In the RM43 model, on the other hand, the additional valence orbitals required a larger box radius of $40\,a_0$, and because of the much larger number of channels we restricted the calculation to 20 continuum orbitals per angular momentum. Consequently, the RM43 model could only yield results for incident energies up to 30 eV. The diagonal elements of the hamiltonian matrix were adjusted to ensure agreement with the experimental excitation thresholds and therefore to allow for a direct comparison between our predictions and the experimental data. The adjustment was performed in such a way that the shift of the states with configuration $5p^5 6p$ was kept as small as possible. Finally, the flexible asymptotic R-matrix (FARM)

package of Burke and Noble [14] was used to calculate the transition matrix elements at each collision energy of interest. We summed the numerically calculated contributions from partial-waves of total electronic angular momentum J_t of the projectile + target system up to a maximum value J_t^{max} and estimated the contributions from higher partial waves using a geometric extrapolation scheme if necessary. Specifically, we chose $J_t^{max} = 31/2$ for RM43 and $J_t^{max} = 79/2$ for RM15 and RM11. Note that such high angular momenta require special care with the numerics, especially with respect to the calculation of exchange integrals [13].

In addition to the R-matrix (close-coupling) calculations, we performed calculations using two distorted-wave models labeled DW1 and DW2 below. Both of these models were described in detail by Dasgupta *et al.* [5]. In contrast to some of our previous work, all distorted-wave calculations were performed with the same target descriptions as the RM15 model, with one notable exception: For excitation of the $2p_5$ and $2p_1$ states with total electronic angular momentum $J = 0$, the small mixing coefficients with the ground state configuration ($5p^6$) were ignored in the DW models, and the remaining coefficients were renormalized to preserve their mutual ratio while guaranteeing normalization of the states to unity. Previous experience showed that the theoretical results are strongly dependent on the small mixing coefficient with the ground-state configuration and, moreover, that it is very difficult to obtain this coefficient correctly in an *ab initio* structure calculation with a small configuration-interaction expansion. In fact, best agreement with experiment in DW calculations is often obtained by the procedure outlined above. The R-matrix models, on the other hand, where this renormalization cannot be performed easily because of strict orthogonality requirements between the initial and the final states, typically yield very questionable results for these transitions.

Following previous experience, the static potential of the excited state was used as the distortion potential in both the incident and the exit channel. Finally, we note that DW1 does not include relativistic effects in the calculation of the distorted waves while DW2 does, and DW1 unitarizes the S-matrix while DW2 does not. Generally, neither one of these effects is expected to be important at projectile energies sufficiently high such that channel coupling is no longer a dominant mechanism. With increasing energy, therefore, one would hope that the DW results converge to each other and to the R-matrix predictions obtained with the corresponding target description. This is an important additional test for the consistency of the models and the importance, or lack thereof, of channel coupling.

III. RESULTS AND DISCUSSION

Figures 1−10 exhibit our results for the angle-integrated cross sections for electron-impact excitation of the $2p_{10} - 2p_1$ states in xenon from the ground state $(5p^6)^1S_0$. The predictions from the various theoretical models described in the previous section are compared with the experimental data of Fons and Lin [1]. We label the curves by "RM##", where "RM" stands for R-matrix and "##" indicates the number of coupled states. Similarly, the distorted-wave models are labeled "DW1" and "DW2", respectively.

Instead of commenting on each curve individually, we will concentrate on discussing the more general trends. To begin with, there is overall qualitative agreement between the experimental data of Fons and Lin [1] and many of the models, although in most cases major discrepancies remain regarding the quantitative agreement. These discrepancies sometimes exceed a factor of two, particularly when the cross sections are relatively small. The curves from the two DW calculations generally come together around 30 eV incident energy. For lower energies, the lack of unitarization in DW2 typically results in much too large cross sections.

Note that all these transitions are optically forbidden, and that we represent each state in an "intermediate-coupling scheme" as a linear combination of singlet and triplet states. Following Henry[15], the cross sections should therefore fall off with increasing incident energy E according to

$$\sigma(E) \propto a/E + b/E^3 \tag{1}$$

Here the coefficient a originates from contributions of spin-allowed but parity and/or orbital angular momentum forbidden transitions, while the coefficient b accounts for spin-forbidden, i.e., pure exchange transitions. As can be seen in the graphs, the cross sections indeed decrease with incident energy beyond the maximum, but the predicted decrease is often quite different in the theoretical curves and the experimental data. The DW calculations effectively correspond to a 2-state RM model containing only the initial and final states. Consequently, if the RM and DW results converge towards each other, this indicates that coupling to channels other than the initial and final ones (often referred to as "higher-order effects") are not important. Assuming the experimental data are reliable, the fact that the RM and DW results do not converge therefore suggests a dominant influence of higher-order processes. This conclusion is also supported by the fact that the RM15 results sometimes

differ significantly from the RM43 predictions. The differences are most pronounced for incident energies below 30 eV. Although this is the highest energy for which RM43 calculations were performed, one can see in most cases the general trend for the curves from the two RM models to approach each other at higher energies. Such a convergence indicates that the additional channels in the RM43 model, compared to RM15, have a diminishing effect on the current results at higher energies. At the present time, of course, we cannot rule out that coupling to other channels, in particular the ionization continuum, may be important as well. This possibility, as well as the effect of the target-structure description, will be further investigated in the future. In a few cases, the DW results converge to the RM15 predictions already around 15 eV incident energy. For most of the transitions, however, it appears that this convergence, if at all, will not occur until well above 200 eV. Even for these optically forbidden transitions, the importance of higher-order effects for such high energies might seem surprising.

Next, it is worth commenting once more on the results for the $J = 0 \rightarrow J = 0$ transitions, i.e., excitation of the $2p_5$ and $2p_1$ states from the ground state $(5p^6)^1S_0$. As already mentioned above, the results are typically very sensitive to the mixing coefficient corresponding to the ground-state configuration in the excited state. Such a coefficient is more reminiscent of a direct process such as elastic scattering (despite the energy loss) than to a strongly forbidden transition. Indeed, this interpretation is supported by the experimental data, which exhibit the maximum at a higher incident energy than for all the other transitions. For these transitions, the two distorted-wave models and RM43 come fairly close at least to the shape but not the magnitude of the experimental cross section data. However, given the fact that the critical mixing coefficient is simply dropped in DW and there are enormous differences between the RM43 and RM15 results, with the latter being unphysically large, any "agreement" between theory and experiment is likely more fortuitous than justified by the current treatments.

We finish with the discussion of a few selected examples showing the similarity, of lack thereof, between the close-coupling and the DW results at high energies. As seen already in the comparisons above, there often remain significant differences between the R-matrix results and the first-order perturbative DW predictions. In fact, only rarely is there a clear trend for the DW results to converge to the corresponding RM curves with increasing energy. Such a convergence would allow for a relatively smooth connection between the

curves obtained with the different collision models. It would also dramatically reduce the computational effort required, since the DW calculations are much less CPU demanding than an RM-model, particularly if the latter has to be pushed to higher energies. In previous work on electron collisions with argon and krypton, we indeed often found convergence between RM and DW results, most importantly for optically allowed transitions where contributions from many partial waves are required. Such a smooth curve is highly desirable for the use of these results in modeling applications.

Figure 11 shows a comparison of the DW results with predictions from the RM15 and RM11 models for excitation of the $2p_{10}$, $2p_9$, and $2p_8$ states (see also figures 1−3). These three cases are typical representatives of what can happen. For the $2p_{10}$ state, the RM11 curve nicely joins up with the two DW curves around 120 eV incident energy, while the RM15 model predicts significantly bigger (almost an order of magnitude) cross sections. These theoretical results indicate that excitation of the $2p_{10}$ state at these high energies mostly occurs through higher-order processes, with the $(5p^5 6s)$ states representing important intermediate steps, rather than through a direct first-order process. From a practical point of view, however, this particular finding may not be too critical, since all models predict very small cross sections for this case, in agreement with the experimental findings (see figure 1).

Channel coupling also seems to be important for excitation of the $2p_9$ state at high energies, except this time the $(5p^5 6s)$ are far less important than for the previous transition. Here RM11 and RM15 yield very similar results at high energies, but again very different from those obtained in the first-order DW models. In this case, the RM results are clearly supported by experiment, with the measured cross sections even slightly bigger than predicted (see figure 2). Finally, the pure exchange transition $(5p^6)^1S_0 \rightarrow 2p_8$ ($^3D_3$) exhibits a different pattern again. Here the DW and RM results are much closer over nearly the entire energy range, and the agreement with experiment is at least satisfactory (see figure 3).

IV. SUMMARY AND OUTLOOK

We have presented several sets of theoretical results for electron impact-excitation of the $(5p^5)6p$ states in xenon from the ground state $(5p^6)^1S_0$. Despite the remaining disagreement between the predictions and the most recent and likely most reliable set of experimental data, the current set of numbers seems usable, though with great care, in modeling applications,

which not only need data for these transitions but also between many excited states that are difficult if not impossible to access with current experimental technology. Hence, comparison between theoretical predictions and the limited set of available experimental data is most important in order to assess the quality of the numerical results. For such applications, it will likely be necessary to either combine the close-coupling results for low incident energies with distorted-wave results at the high energies, or to extrapolate the close-coupling predictions using the known asymptotic energy dependence. The present work indicates that the latter procedure might be preferable for optically forbidden transitions like the ones investigated here, because of remaining higher-order effects not accounted for in the DW approaches. Work towards generating such a set of collision data is currently in progress at the Naval Research Laboratory [16].

In order to obtain more accurate and reliable theoretical results, it seems absolutely critical to improve upon the target description, particularly with regard to the flexibility in the one-electron orbitals. The traditional method of using pseudo-orbitals to account for some of the term dependence in these orbitals does not seem to be a viable approach for this collision problem, especially in light of the many known problems associated with pseudo-orbitals. A very promising alternative lies in the extension of a B-spline R-matrix method [17, 18], particularly when combined with the possibility of using non-orthogonal one-electron target orbitals, as described by Zatsarinny and Froese Fischer [18]. In light of the computational complexity associated with the latter approach, the non-orthogonality may need to be restricted to the most critical valence and outer core orbitals. Also, we expect the flexibility of B-splines and the lack of need for a Buttle correction to be very beneficial from a numerical point of view. These possibilities are currently being explored at Drake University. Initial results for the e−Ne collision system are very promising [19].

Acknowledgments

We would like to acknowledge the contributions of Dr. A.N. Grum-Grzhimailo to the structure calculation. One of us (K.B.) would like to thank Dr. O. Zatsarinny for valuable discussions of this problem. This work was supported, in part, by the National Science Foundation under grants PHY-0244470 (K.B.) and PHY-0070872 (D.H.M), and by the Office

of Naval Research (A.D.).

---

[1] J.T. Fons and C.C. Lin, Phys. Rev. A **58** 4603 (1998).

[2] S. Nakazaki, K.A. Berrington, W.B. Eissner, and Y. Itikawa, J. Phys. B **30** 5805 (1997).

[3] S. Nakazaki, K.A. Berrington, W.B. Eissner, and Y. Itikawa, J. Phys. B **30** L59 (1997).

[4] A.N. Grum-Grzhimailo and K. Bartschat, J. Phys. B **35** 3479 (2002).

[5] A. Dasgupta, K. Bartschat, D. Vaid, A.N. Grum-Grzhimailo, D.H. Madison, M. Blaha, and J.L. Giuliani, Phys. Rev. A **64** (2001) 052710.

[6] A. Dasgupta, K. Bartschat, D. Vaid, A.N. Grum-Grzhimailo, D.H. Madison, M. Blaha, and J.L. Giuliani, Phys. Rev. A **65** (2002) 042724.

[7] K. Bartschat and V. Zeman, Phys. Rev. A **59** (1999) R2552.

[8] C.M. Maloney, J.L. Peacher, K. Bartschat, and D.H. Madison, Phys. Rev. A **61** (2000) 022701.

[9] D.H. Madison, A. Dasgupta, K. Bartschat and D. Vaid, J. Phys. B **37** (2004), in press.

[10] V. Zeman and K. Bartschat, J. Phys. B **30** (1997) 4609.

[11] V. Zeman, K. Bartschat, C. Noren, and J.W. McConkey, Phys. Rev. A **58** (1998) 1275.

[12] C. Froese Fischer, T. Brage, and P. Jönsson, *Computational Atomic Structure: an MCHF Approach* (Bristol: IOP Publishing, 1997)

[13] K.A. Berrington, W.B. Eissner, and P.H. Norrington, Comput. Phys. Commun. **92** (1995) 290.

[14] V.M. Burke and C.J. Noble, Comput. Phys. Commun. **85** (1995) 471.

[15] R.J.W. Henry, Phys. Rep. **68** (1981) 1.

[16] J.P. Apruzese, J.L. Giuliani, and G.M. Petrov, private communication (2004).

[17] H.W. van der Hart, J. Phys. B **30** (1997) 453.

[18] O.I. Zatsarinny and C. Froese Fischer, J. Phys. B **33** (2000) 313.

[19] O.I. Zatsarinny and K. Bartschat, submitted to J. Phys. B (2004).

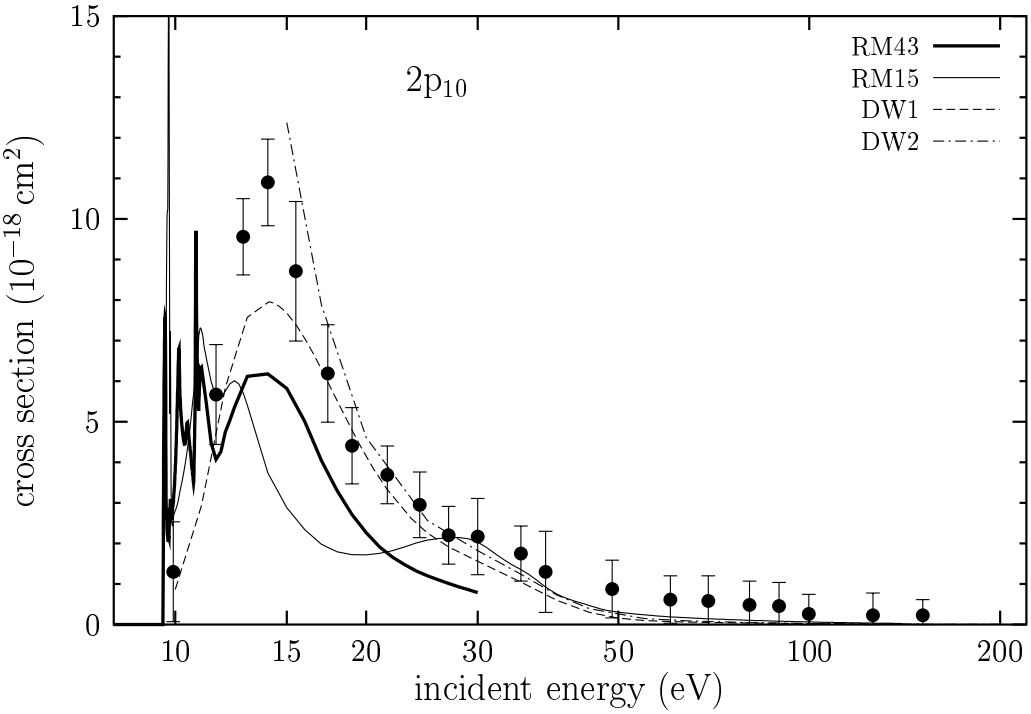

FIG. 1: Angle-integrated cross section for electron-impact excitation of the $2p_{10}$ state in xenon from the ground state $(5p^6)^1S_0$. Predictions from various theoretical models described in the text are compared with the experimental data of Fons and Lin. [1].

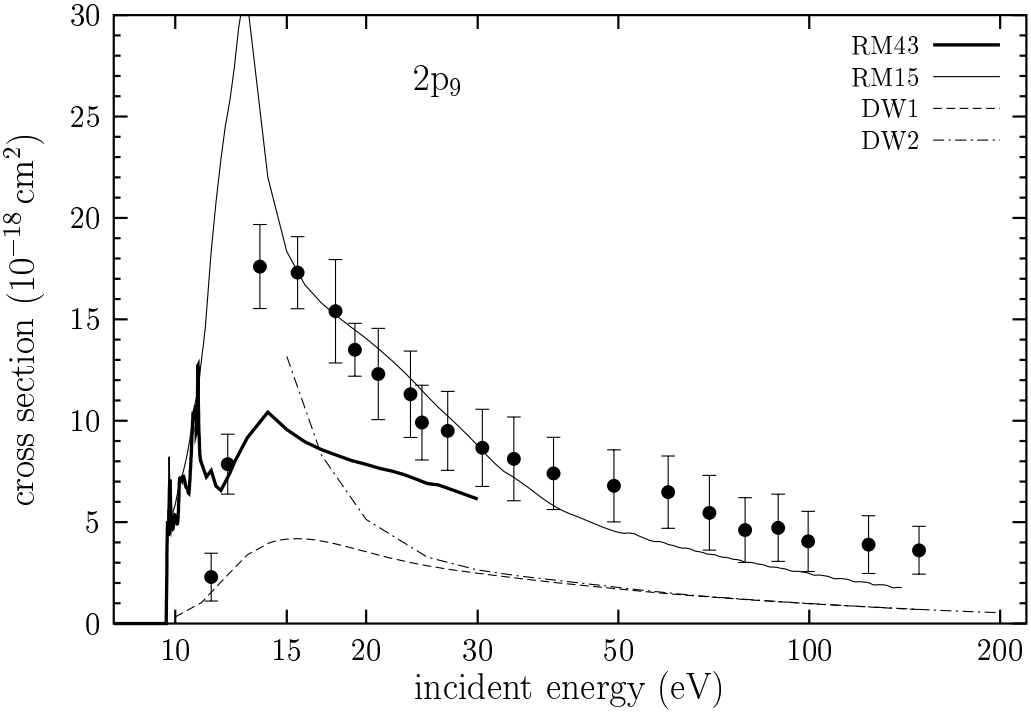

FIG. 2: Same as Fig. 1 for the $2p_9$ state.

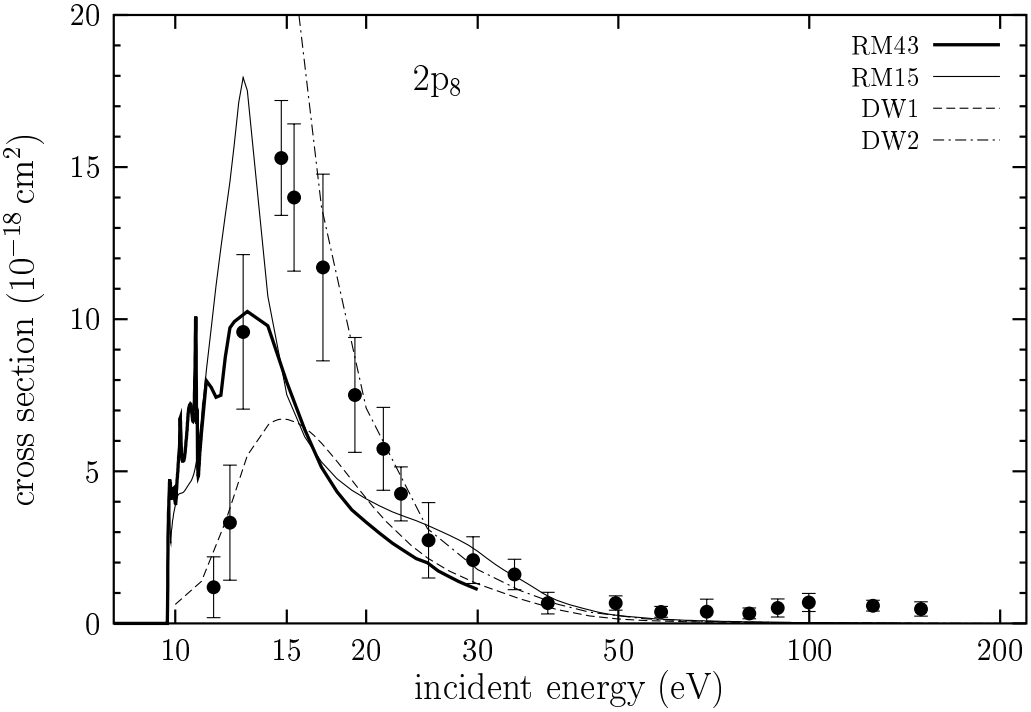

FIG. 3: Same as Fig. 1 for the $2p_8$ state.

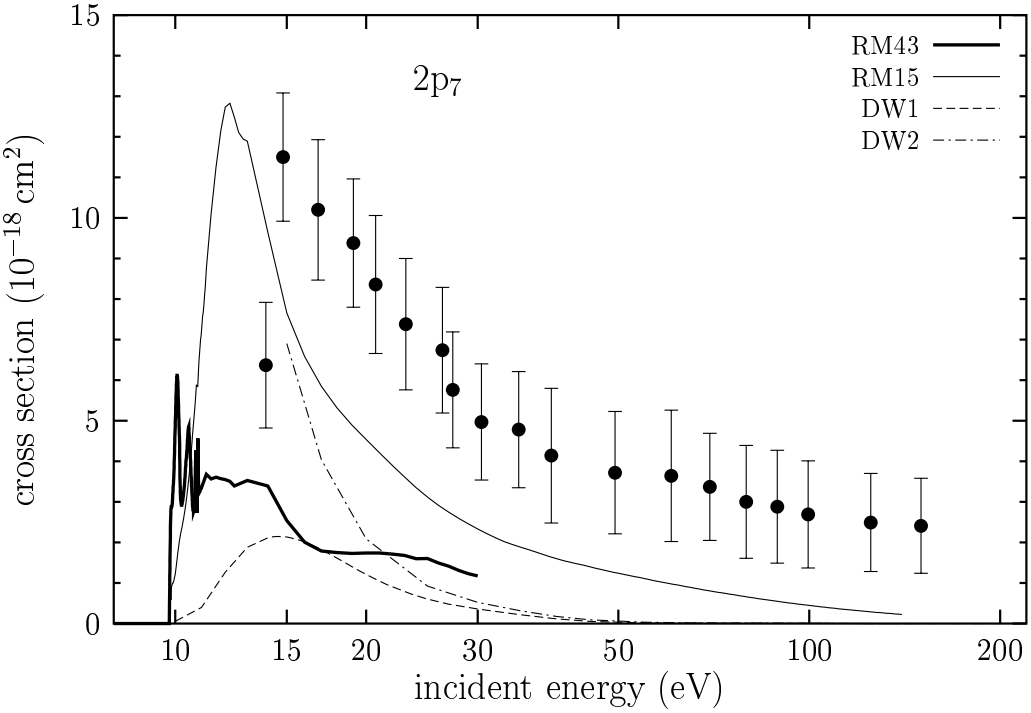

FIG. 4: Same as Fig. 1 for the $2p_7$ state.

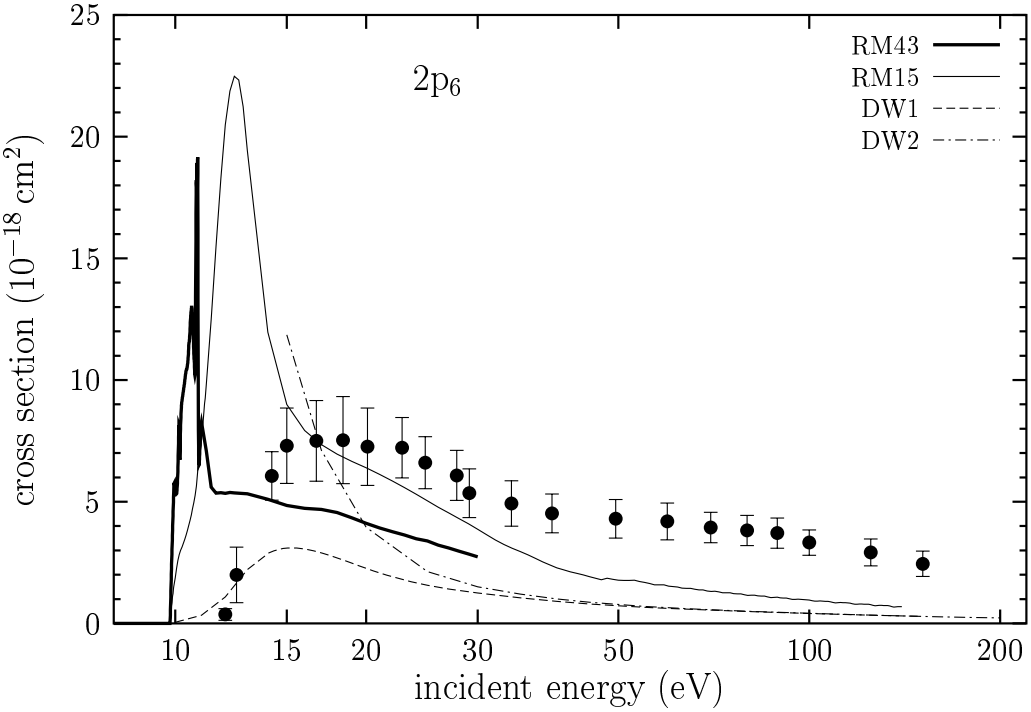

FIG. 5: Same as Fig. 1 for the $2p_6$ state.

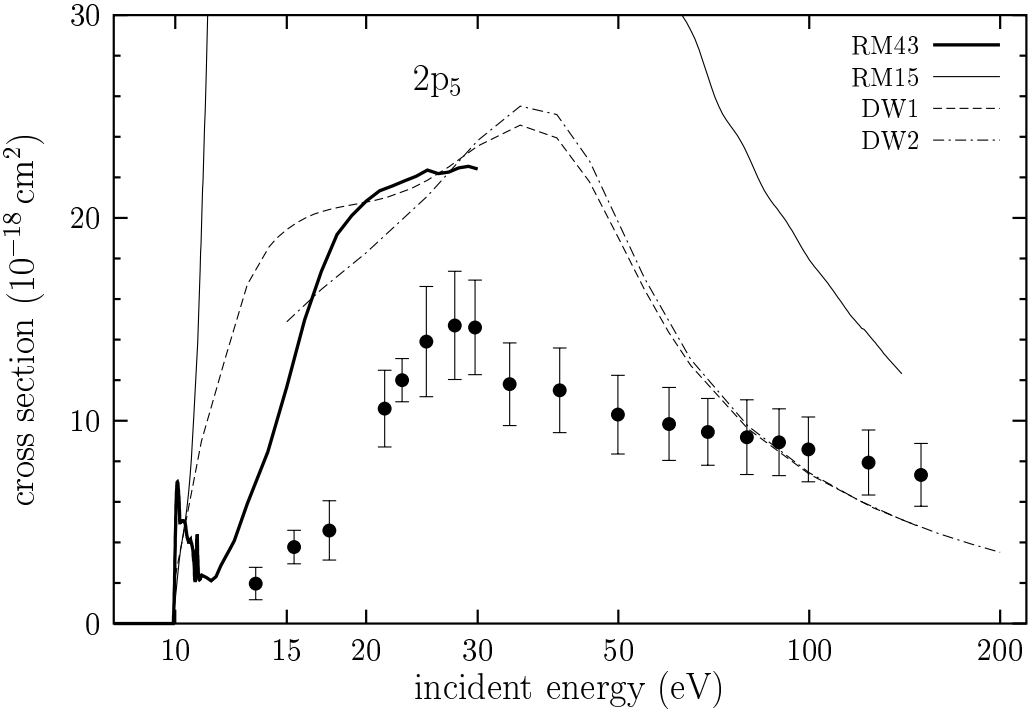

FIG. 6: Same as Fig. 1 for the $2p_5$ state.

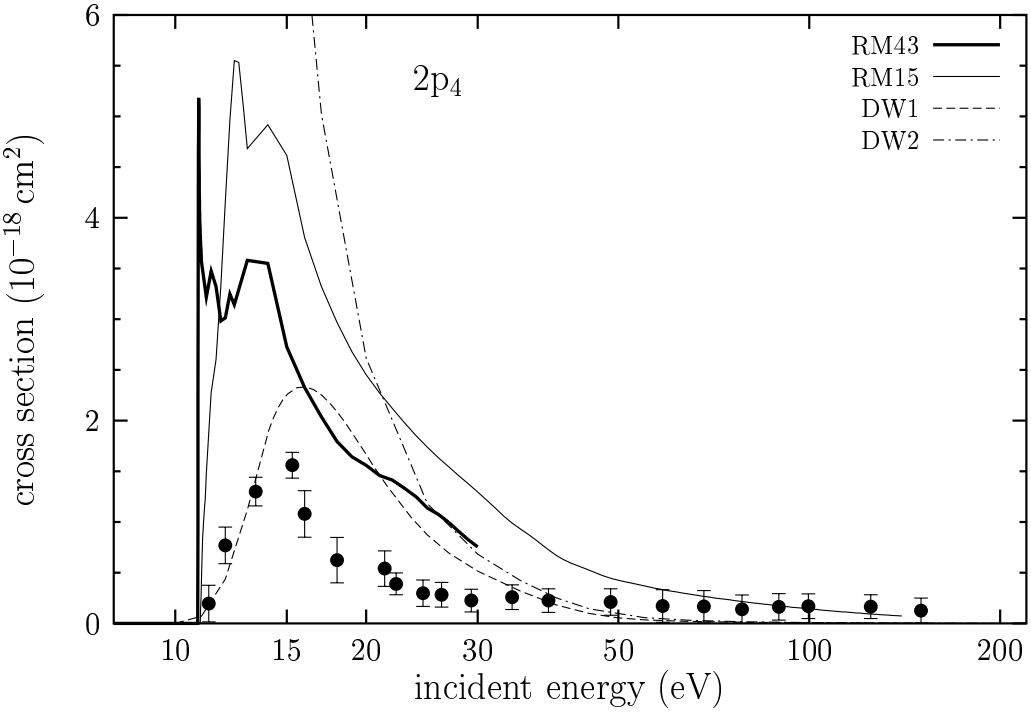

FIG. 7: Same as Fig. 1 for the $2p_4$ state.

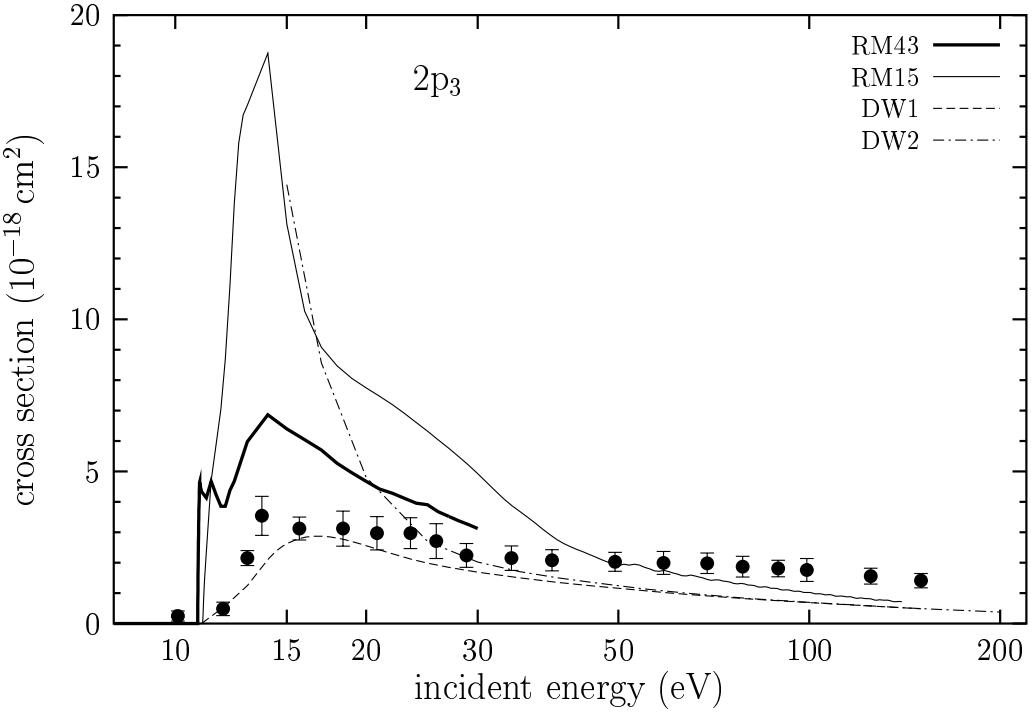

FIG. 8: Same as Fig. 1 for the $2p_3$ state.

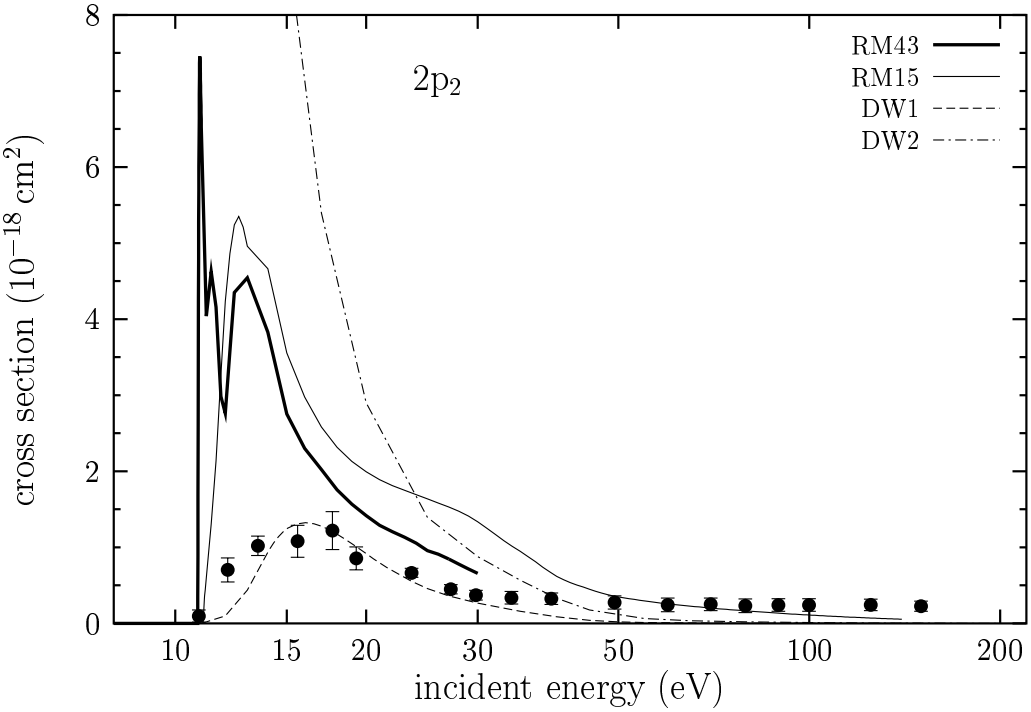

FIG. 9: Same as Fig. 1 for the $2p_2$ state.

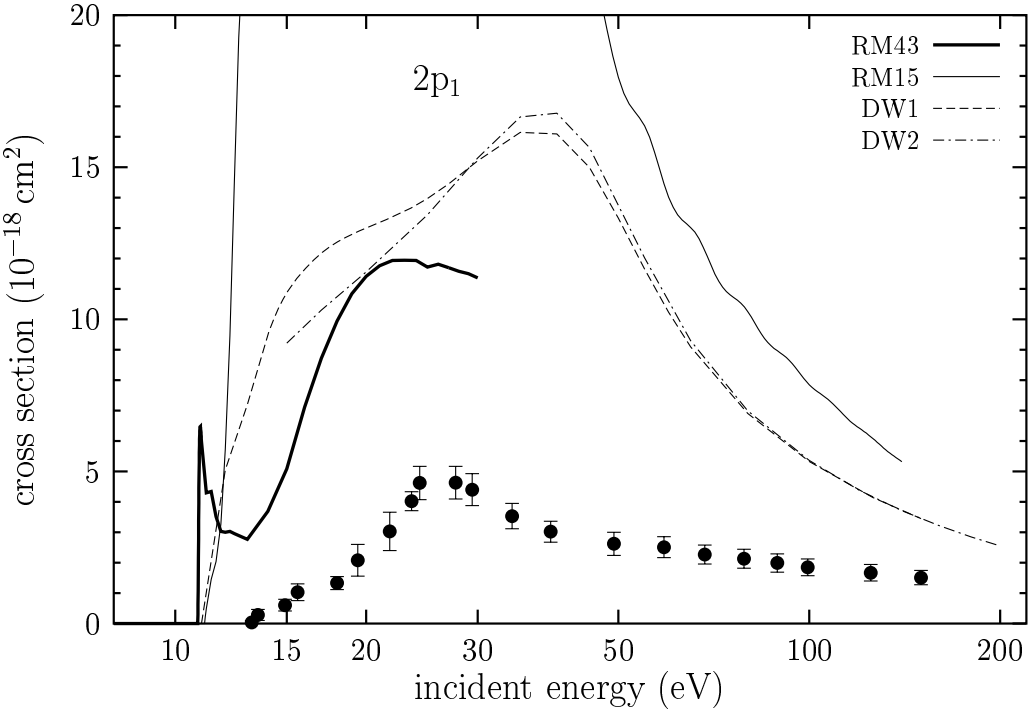

FIG. 10: Same as Fig. 1 for the $2p_1$ state.

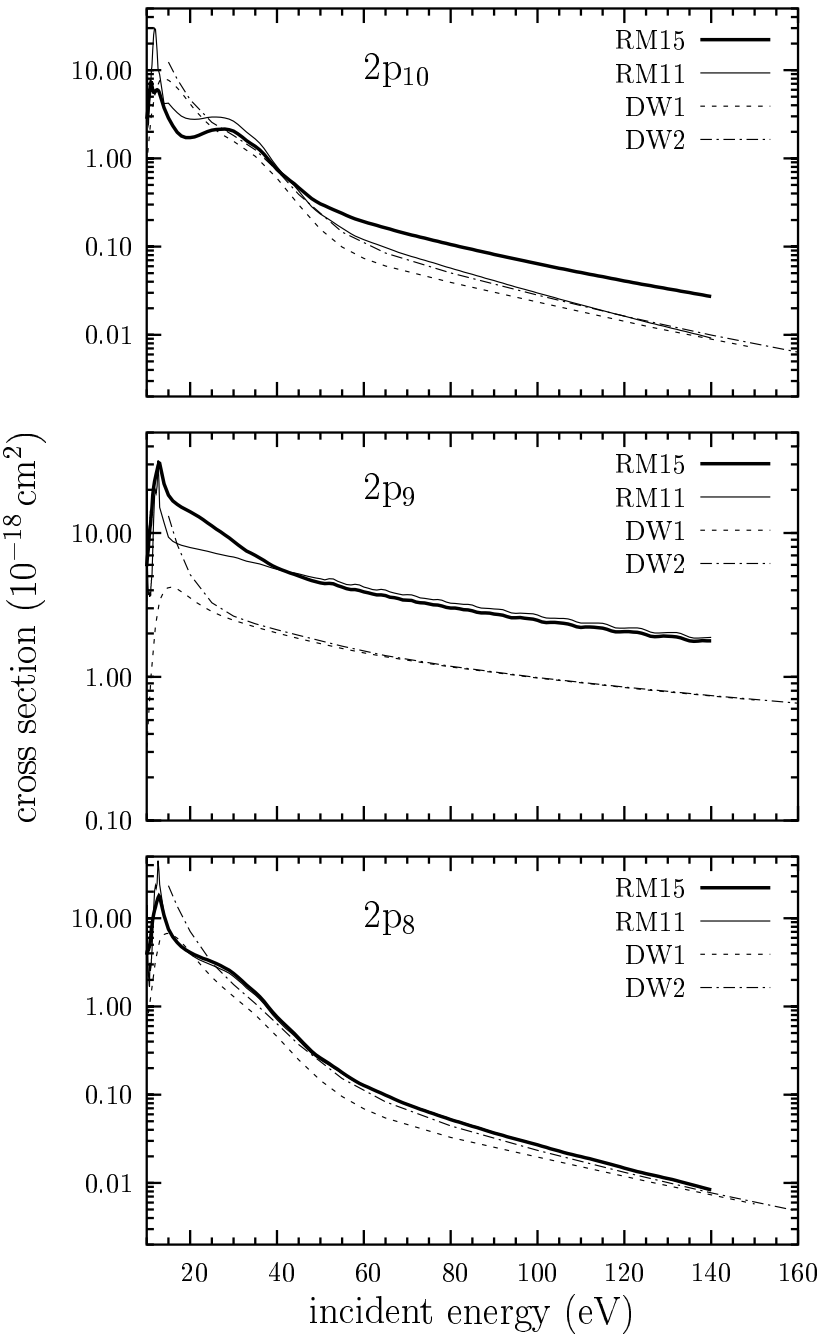

FIG. 11: Angle-integrated cross section for electron-impact excitation of the $2p_{10}$, $2p_9$, and $2p_8$ states in xenon from the ground state $(5p^6)^1S_0$, as obtained in the RM15, RM11, DW1 and DW2 models described in the text.